Second International Symposium on Marine Propulsors
smp'11, Hamburg, Germany, June 2011
Workshop: Propeller performance

The Numerical Predicted of SMP11 Propeller Performance with and without Cavitation

Dengcheng Liu, Fangwen Hong

China Ship Scientific Research Center (CSSRC), Wuxi, China

ABSTRACT
In this paper, the cavitating performance and open water performance of SMP11 propeller was numerically simulated using a hybrid mesh based on RANS solver. A full cavitation model based on transport equation and RNG κ-ε turbulence model were coupled in the RANS solver. The requested thrust and torque coefficient and open water efficiency were present for open water case. The appointed cavity surface and the pressure distribution on the propeller blade for appointed radial sections were present for the cavitation cases. In addition, the added results were given for analyzing propeller cavitating performace.

Keywords
Propeller, Open water, Cavitating, Numerical simulation.

1 INTRODUCTION

Cavitating flows are highly complicated because it is a rapid phase change phenomenon, which often occurs in the high-speed or rotating fluid machineries. It is well known that the cavitating flow raise up the vibration, the noise and the erosion. Therefore, the research on the cavitating flow is of great interest.

Numerical method is highly important approach for studying the cavitating flow. Computational methods for cavitation have been studied since over two decades ago. In general, the methods can be largely categorized into two groups: single-phase modeling with cavitation interface tracking and multi-phase modeling with cavitation interface capturing.

The former approach has been widely adopted for inviscid flow solution methods, such as potential flow boundary element methods. It assumes that the cavitation region is a large bubble with a distinct liquid/vapor interface. Basically three assumptions are made for a cavitation bubble: the bubble boundary is a free surface; the pressure inside the bubble is constant and equals to the saturated vapor pressure of its corresponding liquid; the closure region of the bubble can be approximated by a wake model. Third assumption is prime limitation of the method. The computations are done only for the liquid phase; grid is often regenerated iteratively to conform to the cavity shape. This method is capable of simulating sheet cavitation but may not be adequate for cases in which bubble growth and detachment exists. In addition, so far, they are limited to two dimensional planar or axisymmetric flows because of the difficulties involved in tracking three dimensional interfaces. Kinnas and Fine (1993) developed non-linear boundary element method based on speed potential, and so on.

The latter approach can be adopted for viscous flow solution methods, such as the RANS equation solvers, and is very popular in the cavitation research recently. The cavitating flow is treated as the homogeneous equilibrium single-fluid flow which satisfies Navier-Stokes equation. The key challenge is how to define the mixed density of the single-fluid. In general, the cavitation modeling can be largely categorized into two groups according to the relationship that defines the variable density field. One cavitation modeling is based on the equation of state that relates pressure and density. By assuming the cavitating process to be isothermal, mixed density is simply a function of local pressure. Hoeijmakers and Kwan (1998) adopted a sine law to simulate the cavitating flow around two dimensional hydrofoil with Euler equation, and the computational results of surface pressure coefficient are agreement with experimental data well. Chen and Heister (1996) derived a time and pressure dependent differential equation for density. Qiao Qin (2003) used fifth order polynomial of pressure to define the mixed density. The other cavitation modeling is to introduce the concept of volume fraction, and then the mixed density is calculated using the volume fraction. Kubota et al (1992) coupled the Rayleigh-Plesset equation to compute the volume fraction based on the bubble radius. A mass transport equation cavitation model has been recently developed. Merkle et al (1998), Senocak and Shhy (2001 , 2002), Singal et al (2002), Kunz et al (2000) have employed similar idea based on this concept with differences in the source terms. Niklas et al (2003) simulated two and three dimensional cavitating flow around hydrofoil by solving LES solver with mass transport equation cavitation model which is developed by Kunz. Shin Hyung Rhee and Kawamura

(2003) studied the cavitating flow around a marine propeller using an unstructured mesh with FLUENT 6.1. The cavitating propeller performance as well as cavitation inception and cavity bubble shape were in good agreement with experimental measurements and observation. In addition, Francesco Salvatore (2003) developed a hybrid viscous/inviscid approach for the analysis of marine propeller cavitation. Coutier-Delgosha et al (2003) computed cavitating flows around 2D foil by modifying turbulence model, and the sheet cavity length and the dynamic shedding behaviour were very similar to those observed in the experiment. D.Q.Li(2008) and Dengcheng Liu(2010) predicted unsteady cavitating flows of 3D foil using the same idea. Dengcheng Liu(2008) predicted propeller sheet cavitation using the same idea, and the effect of non-condensable gas mass fraction on predicted cavity shapes was mainly studied.

In this paper, the cavitating performance and open water performance of SMP11 propeller was numerically simulated. The requested data of SMP11 workshop were given.

2 NUMERICAL METHOD

We used a commercial CFD code FLUENT which employs a cell-centered finite volume method based on unstructured mesh and full cavitation model. The SST k-ω turbulence model in non-cavitating cases and the standard k-ω turbulence model in cavitating cases were chosen. Convection terms are discretized using a second order accurate upwind scheme, while diffusion terms are discretized using a second order accurate central differencing scheme. A segregated solver with SIMPLE as the velocity-pressure coupling algorithm was selected. The discrete equations are solved using pointwise Gauss-Seidel iterations, and algebraic multi-grid method accelerates the solution convergence.

2.1 Governing Equations

For the multi-phase flow solutions, the single-fluid mixture model is employed. The governing equations are written for the mass and momentum conservation of mixture fluid as follows:

$$\frac{\partial(\rho_m)}{\partial t}+\frac{\partial(\rho_m u_i)}{\partial x_i}=0 \tag{1}$$

$$\frac{\partial(\rho_m u_i)}{\partial t}+\frac{\partial(\rho_m u_i u_j)}{\partial x_j}=-\frac{\partial p}{\partial x_i}+\frac{\partial}{\partial x_j}\left[(\mu+\mu_t)\left(\frac{\partial u_i}{\partial x_j}+\frac{\partial u_j}{\partial x_i}\right)\right] \tag{2}$$

Where ρ_m is the mixed density , μ is the mixed viscosity, μ_t is the mixed eddy viscosity.

2.2 Full Cavitation Model

The mixed density is controlled by vapor volume fraction f:

$$\frac{1}{\rho_m}=\frac{f}{\rho_v}+\frac{f_g}{\rho_g}+\frac{1-f-f_g}{\rho_l} \tag{1}$$

The vapor transport equation is written as:

$$\frac{\partial(\rho_m f)}{\partial t}+\nabla\bullet\left(\rho_m \overline{V} f\right)=\nabla\bullet\left(\mu_t \nabla f\right)+R_e-R_c \tag{4}$$

Where ρ_v , ρ_g and ρ_l are the density of vapor, non-condensable gas and liquid, respectively. R_e and R_c are the rates of vapor generation and condensation, respectively. To solve the Equation, R_e and R_c need to be given. Singhal et al (2002) derived the expressions.

$$R_e=-C_e\frac{\sqrt{k}}{S}\rho_l\rho_v\left(\frac{2}{3}\frac{p_v-p}{\rho_l}\right)^{1/2}(1-f_v-f_g) \quad \text{if } p<p_v \tag{5}$$

$$R_c=C_c\frac{\sqrt{k}}{S}\rho_l\rho_l\left(\frac{2}{3}\frac{p-p_v}{\rho_l}\right)^{1/2}f_v \quad \text{if } p>p_v \tag{6}$$

Where p_v is saturated vapor pressure. C_e and C_c are two empirical constants and k is the local turbulent kinetic energy. Singhal et al. (2002) used 0.02 and 0.01 for C_e and C_c , respectively, after careful study of numerical stability and physical behavior of the solution. Their values are adopted in the present study. S is surface tension. f_g is non-condensable gas mass fraction.

3 COMPUTATIONAL CONDITION

3.4 Geometry model and the cases

In this paper, the research object is a five bladed SMP11 propeller. It is a controllable pitch propeller with diameter D=0.250m, hub diameter ratio of 0.3, pitch-to-diameter ratio of 1.635 at 0.7 radial section, skewed angle of 19.12° and area ratio of 0.78. Table 1 is the cases of open water computational. Table 2 is the cases of cavitation computational. J is advance ratio which is determined according to the thrust identity with noncavitating condition. N is rotational speed of propeller. σ is cavitation index. The expression of cavitation index, thrust and torque coefficient is written as follow:

$$\sigma=\frac{P_\infty-P_v}{\frac{1}{2}\rho_l(ND)^2}, \quad Kt=\frac{T}{\rho_l N^2 D^4}, \quad Kq=\frac{Q}{\rho_l N^2 D^5} \tag{7}$$

Table.1 the cases of open water computational

Water density(kg/m^3)	998.2
Viscosity of water(kg/m-s)	1.003e-3
Rate of revolutions(1/s)	15

Table.2 the cases of cavitation computational

case	*Kt*(no cav)	*J*	σ	*N*
2-3-1	0.387	1.025	2.024	25
2-3-2	0.245	1.287	1.424	25
2-3-3	0.167	1.428	2.000	25
Water/Vapor density(kg/m^3)			997.44/0.01927	
Viscosity of water/Vapor(kg/m-s)			1.003e-3/8.8e-6	

3.5 Computational mesh and conditions

For steady flow simulation, the computational domain was created as one passage surrounding a blade: inlet at 3D upstream; exit at 4D downstream; solid surfaces on the blade and hub, centered at the coordinate system origin and aligned with uniform inflow; outer boundary at 3D from the hub axis; and two rotationally periodic boundaries with 72°angle in between. A hybrid mesh was generated using GAMBIT. The blade surface was meshed with triangles. The region around the root, tip and blade edges was meshed with smaller triangles, and the inner region was filled with appropriately growing triangles. Although the computational regions are different between open water and cavitation case due to different hub, the mesh are similar. The number of tetrahedral cells was about 658,000. The remaining region in the domain was filled with hexahedral cells, and the number of hexahedral cells was about 48,000.

Boundary conditions were set to simulate the flow around a rotating propeller: on the inlet boundary and the outer boundary, velocity components of uniform stream with the given inflow speeds were imposed which is calculated by advance coefficient; on the blade and hub surface, the no slip condition was imposed; and on the periodic boundaries, rotational periodicity was ensured; on the exit boundary, the static pressure was set to a constant value, zero in non-cavitating cases, while the static pressure is determined by cavitation index in the cavtating cases, while other variables were extrapolated.

4 RESULTS

4.1 Open water performance

Table 3 presents the predicted thrust and torque coefficient. When thrust coefficient is equal to zero, the advance coefficient is 1.673 which is close to pitch ratio of 1.635 at 0.7 radial section, this is reasonable because the life angle of propeller at this condition is close to zero.

Table.3 predicted open water performance

J	Kt	10Kq	ETA0
0.400	0.7305	1.6387	0.2838
0.600	0.6158	1.4239	0.4130
0.800	0.5055	1.223	0.5263
1.000	0.3971	1.0215	0.6187
1.200	0.2887	0.8107	0.6801
1.400	0.1779	0.5832	0.6797
1.600	0.0530	0.3104	0.4348
1.673	0.0000	0.1897	0.0000

4.2 Propeller cavitation

We simulated propeller sheet cavitation at three different advance ratio and different cavitation index. When the thrust is equal to appointed value with noncavitating condition, the advance coefficient are not strict equal, but the error is less than 1.5%.

According to my experience, the cavity shape defined by iso-surface of vapor volume fraction of 0.1 will agree well with experiment. So the appointed cavity surface (iso-surface of vapor volume fraction of 0.2, 0.5, 0.8) and cavity surface defined by iso-surface of vapor volume fraction of 0.1 are also given.

Table 4 gives the thrust breakdown due to cavitation. Figure 1~Figure 3 presents the computed cavity shapes of different cases respectively. And the equal radial sections are 0.35r, 0.7r, 0.9r and 0.95r in the figure from root to tip. From Figure 1 we clearly see that cavitation is to occur in the tip, root and leading edge of middle radial section of suction side of propeller at case2-3-1, and the cavitaion area is small at three region, so the thrust breakdown is only 2.359% (see table 4). From Figure 2 and Figure 4(a) we clearly see that there are both face cavitation and back cavitation, and in the tip area and leading edge of middle radial section of pressure side the cavitation is little, at the root region there are serious cavitation both at pressure side and suction side, so the thrust breakdown is highly 20%(see table 4). From Figure 3 and Figure 4(b) we clearly see that there are serious face cavitation at leading edge of most radial section, the same with case2-3-2, there are both face cavitation and back cavitation at root region, and the thrust breakdown is also highly 20%(see table 4).

Figure 5~Figure 7 presents the computed different radial section pressure coefficient of three different cases respectively. For the four radial sections 035, 070, 090 and 095 are possible entries for r/R =0.35, 0.70, 0.90 and 0.95. For the cavitation state ncav and wcav is used in the figure, for the computations of the non-cavitating and the cavitating propeller. From figure 5~figure 7, we known that the pressure distributions of cavitation condition are similar with noncavitating condition at the no cavitation region, and the cavitation only affect the pressure coefficient of occurred cavitation region. Comparing the pressure distribution between noncavitating and cavitating at 0.35 radial section of case2-3-2 and case2-3-3, we also known that the face cavitation and back cavitation occurred at root region, because at this region the pressures of pressure side and suction side are below to vapor pressure. The expression of pressure coefficient is written as follow:

$$C_p = \frac{P - P_0}{\frac{1}{2}\rho_l\left(V^2 + (2\pi Nr)^2\right)} \tag{8}$$

Table.4 thrust breakdown with cavitation

case	σ	Kt(no cav)	Kt(cav)	Error(%)
2-3-1	2.024	0.387	0.374	-3.359
2-3-2	1.424	0.245	0.194	-20.816
2-3-3	2.000	0.167	0.132	-20.958

4 CONCLUSIONS

In this paper, the cavitating performance and open water performance of SMP11 propeller was numerically simulated using a hybrid mesh based on RANS solver. A full cavitation model based on transport equation and RNG κ-ε turbulence model were coupled in the RANS solver. The requested thrust and torque coefficient and open water efficiency were present for open water case. The appointed cavity surface and the pressure distribution on the propeller blade for appointed radial sections were present for the cavitation cases. In addition, the added results were given for analyzing propeller cavitating performace.

REFERENCES

Coutier-Delgosha, O., Reboud, J.L., and Fortes-Patella, R., Evaluation of the Turbulence Model Influence on the Numerical Simulations of Unsteady Cavitation [J], Journal of Fluids Engineering, Vol. 125, Issue 1, pp. 38-45, 2003.

Dengcheng Liu．(2008)． The CFD analysis of propeller sheet cavitation. Proceedings of the 8th International Conference on Hydrodynamics. Nantes France. 2008

Dengcheng Liu．(2010)．The Numerical Research on Unsteady Cloud Cavitating Flow of 3D Twisted Hydrofoil and Compared with Experiment. [J]. Chinese Journal of Hydrodynamics, Vol.25 No.6. 721-726.

Dengcheng Liu, Fangwen Hong．(2010)．The Numerical and Experimental Research on Unsteady Cloud Cavitating Flow of 3D Elliptical Hydrofoil. Proceedings of the 9th International Conference on Hydrodynamics. Shanghai China. 2010

D.Q.Li, Grekula, Prediction of dynamic shedding of cloud cavitation on a 3D twisted foil and comparison with experiments [C], 27th Symposium on Naval Hydrodynamics (Cav2003), Seoul, Korea, Oct. 5-10, 2008

Francisco Pereira et al. 2002. Experimental and Numerical Investigation of the Cavitation Pattern on a Marine Propeller.[C]. 24th Symposium on Naval Hydrodynamics. Fukuoka, Japan, 8-13 July.

Francesco Salvatore et al. 2003. A Viscous/Inviscous Coupled Formulation for Unsteady Sheet Cavitation Modelling of Marine Propellers. [C]. Fifth International Symposium on Cavitation (cav2003) Osaka, Japan, November 1-4.

Hoeijmakers.H.W.M, Janaaens.M.E, Kwan. W. 1998. Numerical Simulation of Sheet Cavitation. [C]. Proceedings of 3rd International Symposium on Cavitation，Grenoble，France.

Inanc Senocak, Wei Shyy. 2001. Numerical Simulation of Turbulent with Sheet Cavitation. [C]. Fourth International Symposium on Cavitation (cav2001), SessionA7.002.

Inanc Senocak, Wei Shyy. 2002. A Pressure-Based Method for Turbulent Cavitating Flow Computation. [J].Journal of Computational Physics. 176,363-383.

Kubota, A., Kato, H., and Yamaguchi, H., 1992. A New Modeling of Cavitating Flows: A Numerical Study of Unsteady Cavitation on A Hydrofoil Section. [J]. J. of Fluid Mechanics, Vol.240, 1992, pp.59-96.

Kunz, R.F., Boger, D.A., Stinebring, D.R., Chyczewski, T.S., Lindau, J.W., Gibeling, H.J., Venkateswaran, S., and Govindan, T.R., 1996. A preconditioned Navier-Stokes method for two-phase flows with application to cavitation prediction,[J]. Computers and Fluids, Vol.29, 2000, pp.849-875.

Kinnas S A, Fine E.A 1993. Numerical Nonlinear Analysis of The Flow Around 3-D cavitating Hydrofoil. [J].Journal of Fluid Mechanics. 254:151-181.

Merkle. C. L, Feng. J, Buelow. P. E. O. 1998. Computational Modeling of the Dynamics of Sheet Cavitation. [C].Proceedings of 3rd International Symposium on Cavitation, Grenoble, France.

Niklas, Christer Fureby. 2003. LES of the Flow past Simplified Submarine Hulls. [C]. The 8th International Conference on Numerical Ship Hydrodynamics. Busan. Korea. September 22-25.

Qiao Qin, Song. C.C.S. 2003. A Virtual Single-phase Natural Cavitation Model and its Application to CAV2003 Hydrofoil. [C]. Fifth International Symposium on Cavitation (cav2003) Osaka, Japan, November 1-4.

Singhal.A.K, Athavale. M.M.. 2002. Mathematical Basis and Validation of the Full Cavitation Model. [J].Journal of Fluids Engineering.Vol.124.617-624.

Shin Hyung Rhee, Takarumi Kawamura. 2003. A Study of Propeller Cavitation Using A RANS CFD Method. [C]. The 8th International Conference on Numerical Ship Hydrodynamics. Busan. Korea. September 22-25.

Yongliang Chen, Heister.S.D.1996. Modeling Hydrodynamic Nonequilibrium in Cavitating Flows. [J]. Journal of Fluids Engineering.Vol.118.172-178.

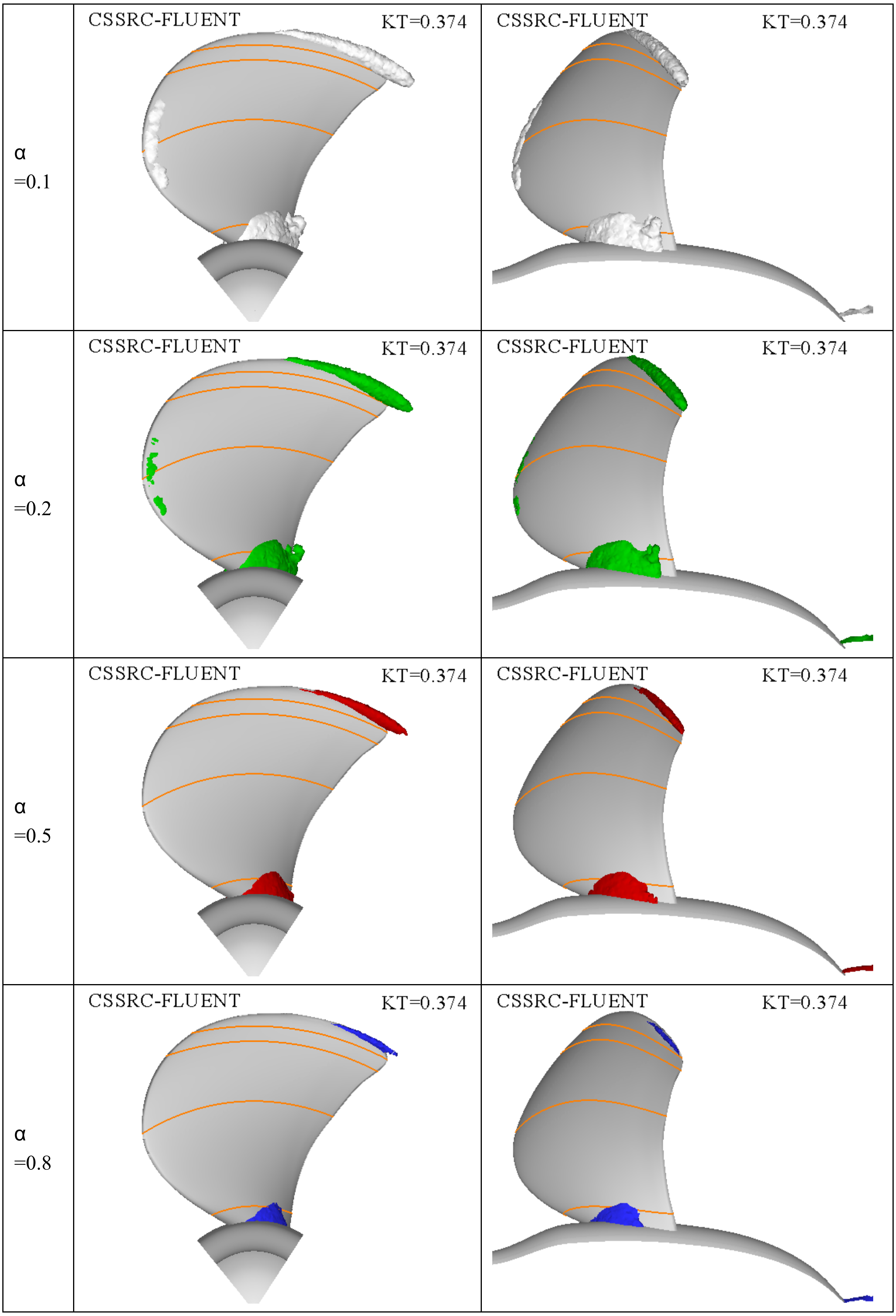

Figure 1 computed cavity shapes of case2-3-1(σ=2.024)

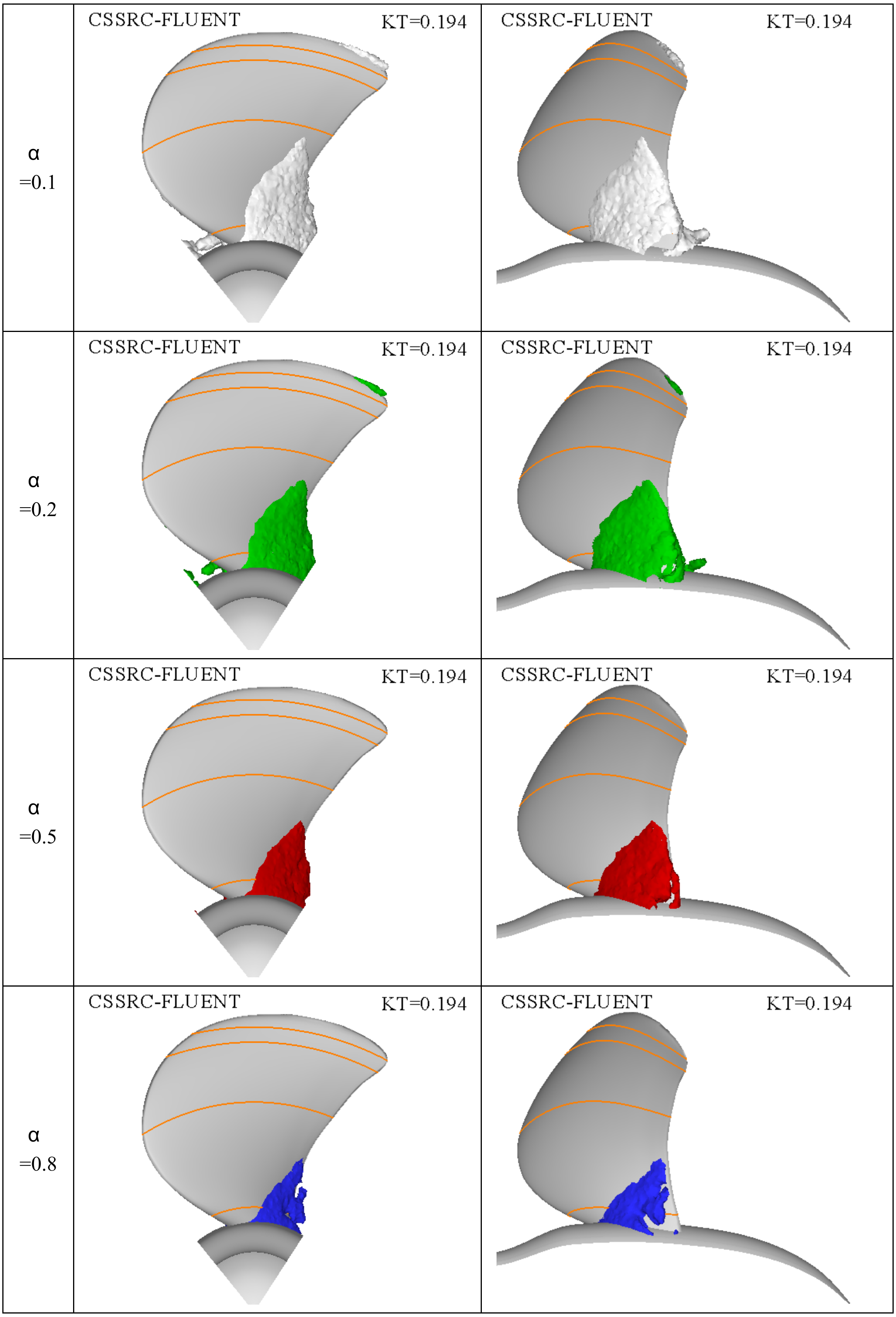

Figure 2 computed cavity shapes of case2-3-2(σ=1.424)

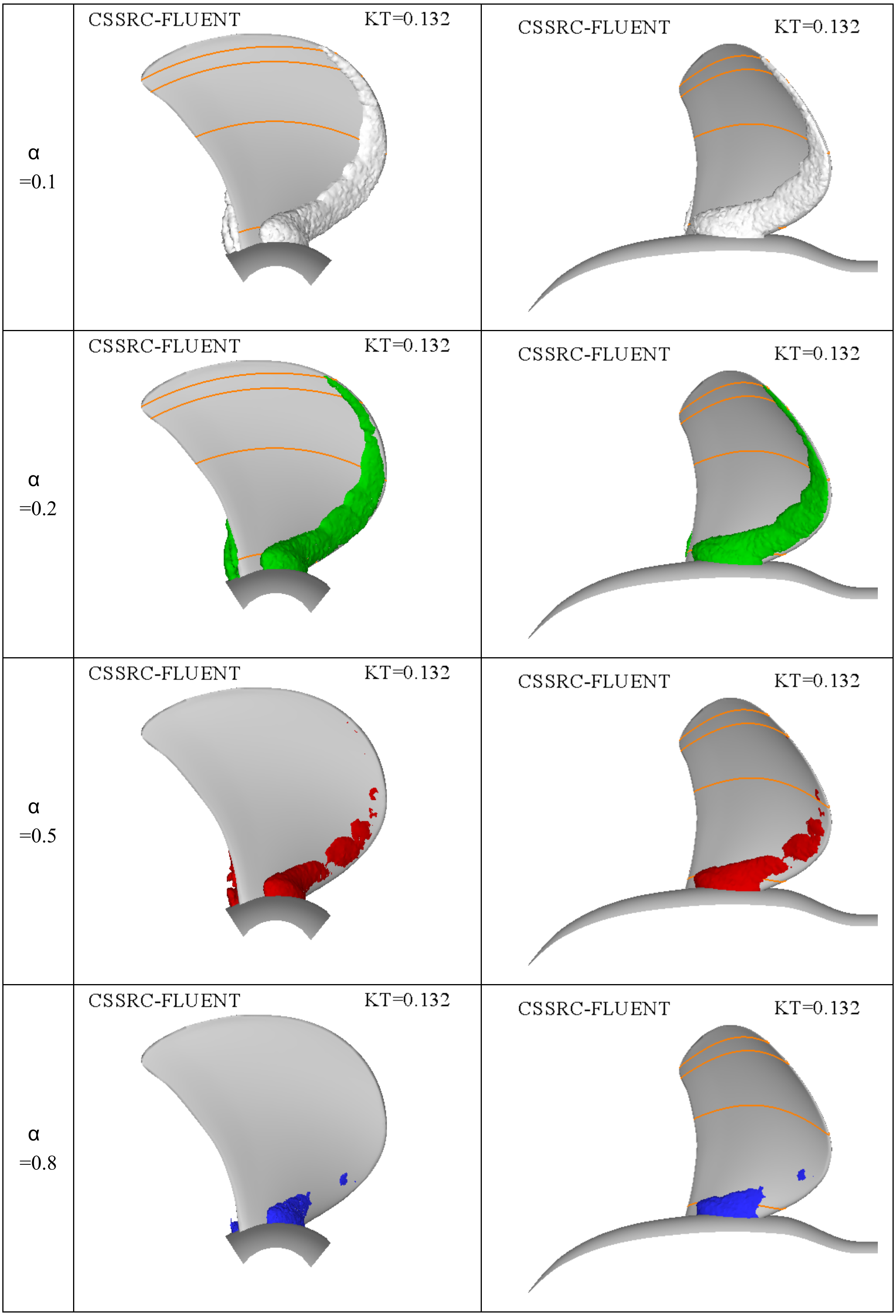

Figure 3 computed cavity shapes of case2-3-3(σ=2.000)

α =0.1	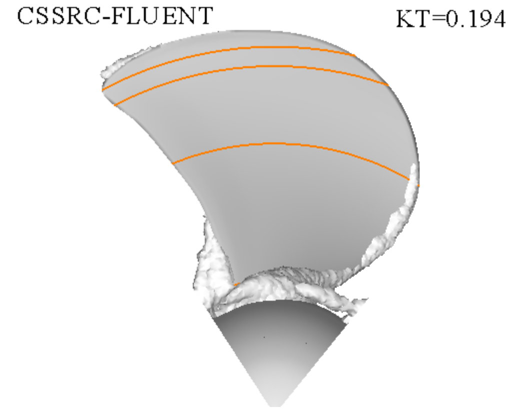	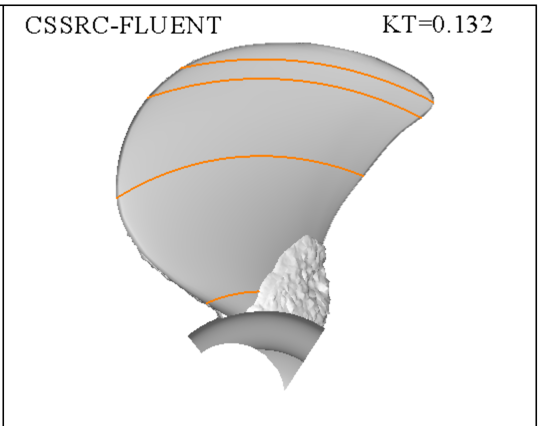
	(a) case2-3-2 suction side	(b) case2-3-3 pressure side

Figure 4 computed cavity shapes of case2-3-2 and case2-3-3

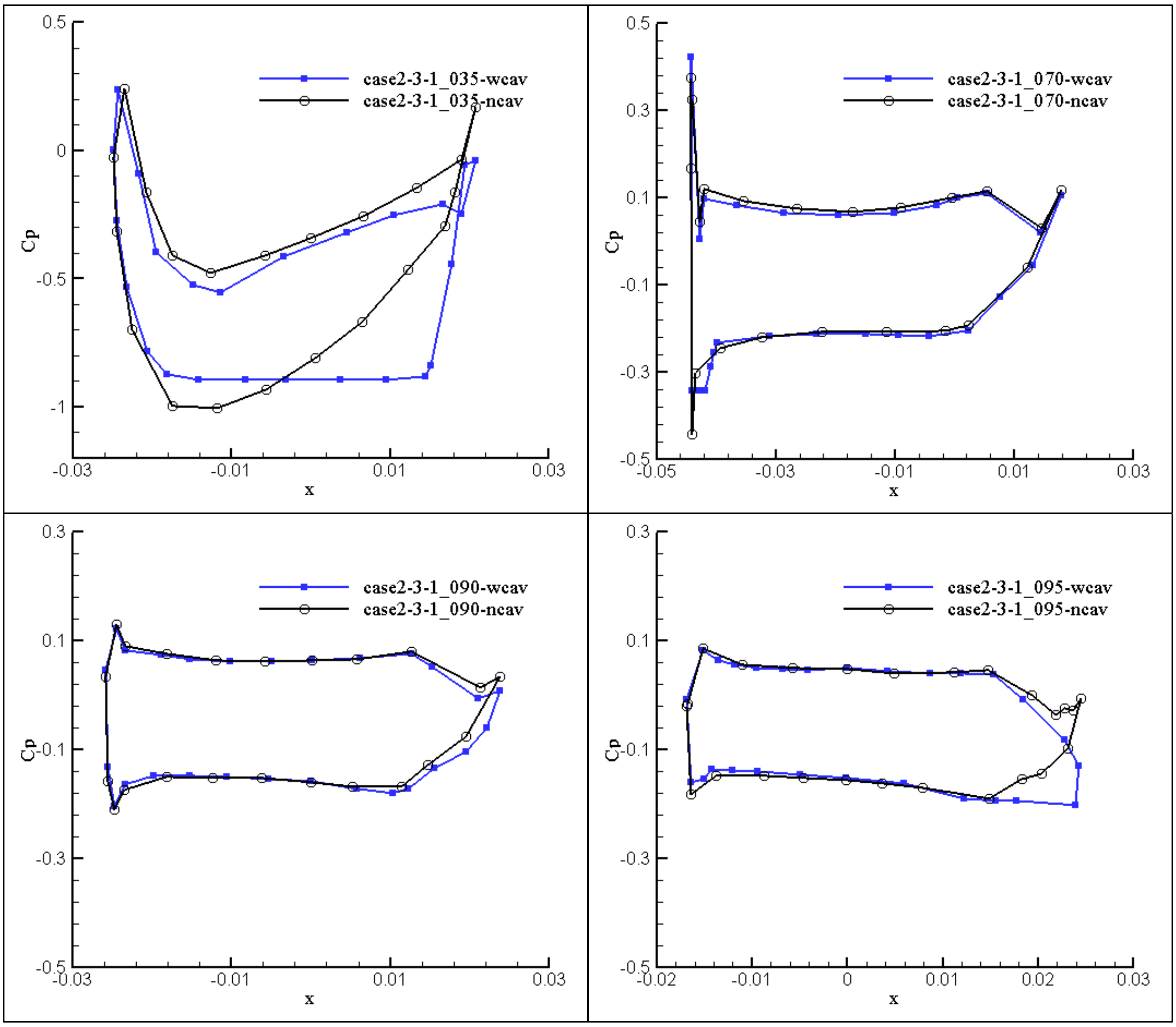

Figure 5 computed different radial section pressure coefficient of case2-3-1

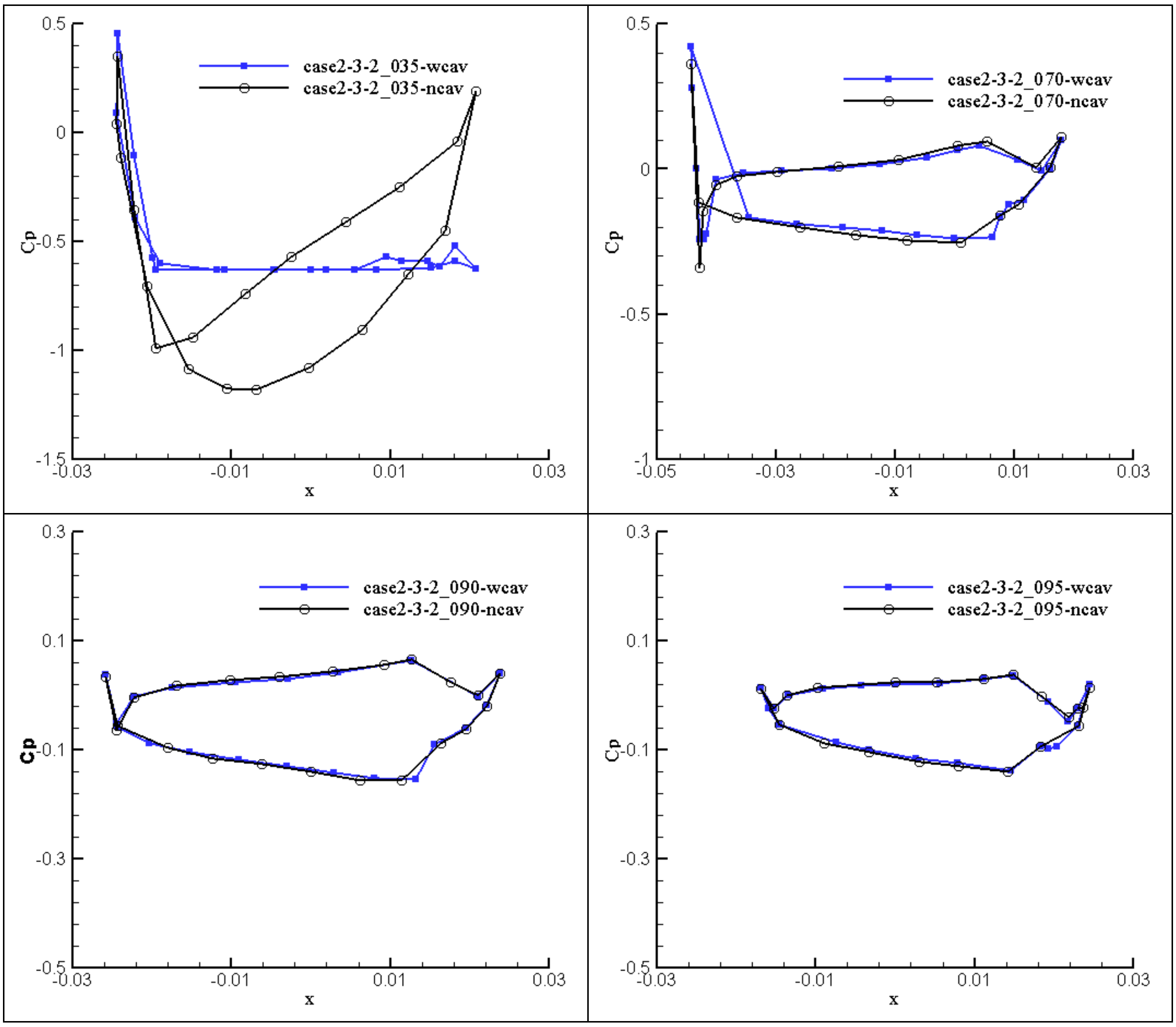

Figure 6 computed different radial section pressure coefficient of case2-3-2

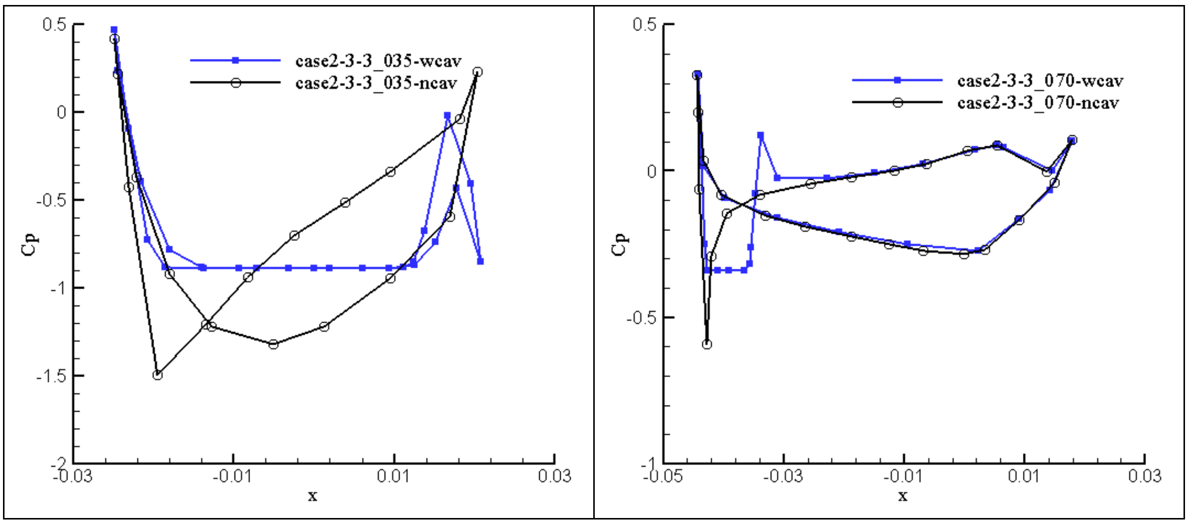

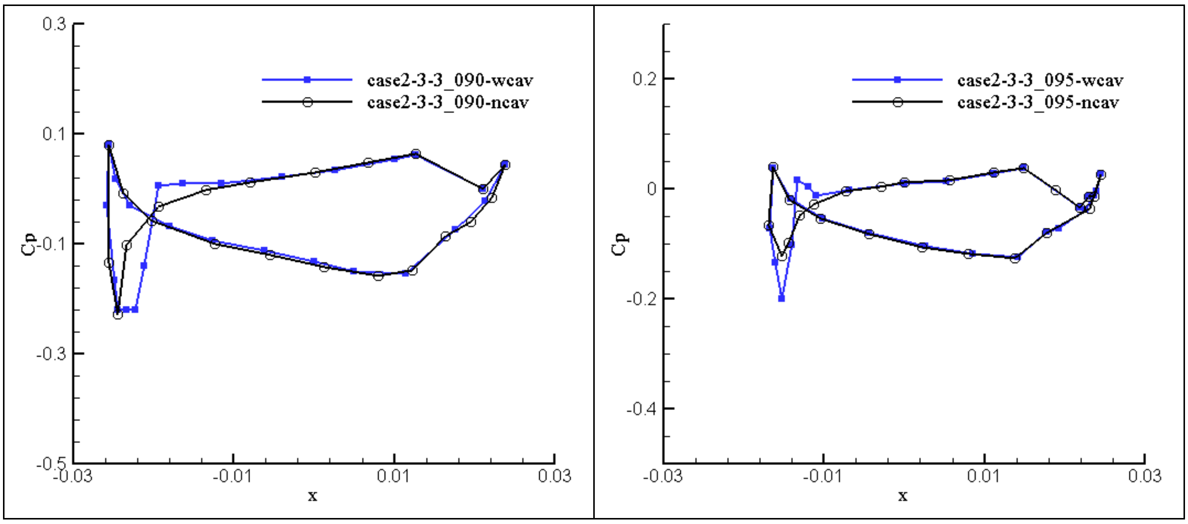

Figure 7 computed different radial section pressure coefficient of case2-3-3